Arthritis Research & Therapy

RESEARCH

Open Access

Akt2 inhibition alleviates temporomandibular joint osteoarthritis by preventing subchondral bone loss

Shi-Yang Feng[1,3,4,5†], Meng-Nan Cao[1,2,3,4,5†], Chen-Chen Gao[1,2,3,4,5], Yi-Xin Li[1,2,3,4,5], Jie Lei[1,3,4,5*] and Kai-Yuan Fu[1,3,4,5*]

Abstract

Background This study aimed to investigate the role and mechanism of the Akt2 pathway in different stages of anterior disc displacement (ADD)-induced temporomandibular joint osteoarthritis (TMJOA).

Methods A rat model for TMJOA that simulates anterior disc displacement was established. For inhibit Akt2 expression in subchondral bone, rats were intravenously injected with adeno-associated virus carrying Akt2 shRNA at a titer of 1×10^{12} transducing units/mL 10 days before the ADD or sham operations. The rats were euthanized and evaluated 1 or 8 weeks after surgery, as these time points represented the early or advanced stage of ADD. Immunostaining was performed to examine the expression and location of phosphorylated Akt2 in different stages of ADD. Microcomputed tomography, hematoxylin and eosin staining, toluidine blue staining, Western blotting, immunohistochemical and immunofluorescence staining were used to elucidate the pathological changes and potential mechanisms underlying ADD-induced TMJOA.

Results In the rat model of ADD-induced TMJOA, rapid condylar bone loss occurred with increased phosphorylation of Akt2 in subchondral bone macrophages within 1 week post-surgery. At 8 weeks after surgery, abnormal remodeling of subchondral bone and degenerative changes in cartilage were observed. Inhibiting Akt2 reduced condylar bone resorption following ADD surgery while improving condylar bone morphology at 8 weeks post-surgery. Additionally, inhibition of Akt2 alleviated cartilage degeneration characterized by a decreased number of apoptotic chondrocytes, reduced expression of matrix metalloproteinases, and increased collagen type II expression in cartilage tissue.

Conclusions The Akt2 pathway is activated mainly in subchondral bone macrophages during the early stage of ADD and plays an important role in regulating subchondral bone remodeling. Inhibition of Akt2 could serve as a prophylactic treatment to slow the progression of ADD-induced TMJOA.

Keywords Temporomandibular disorders, Osteoarthritis, Bone loss, Cartilage degeneration, Akt2 pathway

†Shi-Yang Feng and Meng-Nan Cao contributed equally to this work.

*Correspondence:
Jie Lei
leijierebecca1986@163.com
Kai-Yuan Fu
kqkyfu@bjmu.edu.cn
[1]Center for TMD & Orofacial Pain, Peking University School and Hospital of Stomatology, No. 22 Zhong Guan Cun South Ave, Beijing 100081, China
[2]Central Laboratory, Peking University School and Hospital of Stomatology, Beijing, China
[3]National Center for Stomatology & National Clinical Research Center for Oral Diseases, Beijing, China
[4]National Engineering Research Center of Oral Biomaterials and Digital Medical Devices, Beijing, China
[5]Beijing Key Laboratory of Digital Stomatology, Beijing, China

Background

Osteoarthritis (OA) is one of the most prevalent chronic degenerative diseases, and involves articular cartilage degeneration, subchondral bone remodeling, and synovial inflammation [1]. As a susceptible site of OA, the temporomandibular joint (TMJ) is capable of active bone remodeling and a rapid response to mechanical stimulation [2–5]. The main clinical manifestations of TMJOA include orofacial pain, joint sounds, and limited jaw movements, which severely impact both patients' quality of life and aesthetics [6–8]. Anterior disc displacement (ADD) is considered a major cause of TMJOA [9, 10]. As the pathogenesis of ADD-induced TMJOA has not been fully elucidated, current treatment strategies generally focus on pain relief but not on preventing disease progression. Most patients with advanced-stage TMJOA experience irreversible cartilage degeneration and bone sclerosis and have to undergo joint replacement surgery to restore joint function, resulting in a substantial social and economic burden [11]. Thus, strategies to prevent the progression of TMJOA and improve the structure of the articular cartilage and subchondral bone are urgently needed.

The Akt signaling pathway is sensitive to changes in the microenvironment and is associated with various diseases, including cancer, diabetes, and arthritis [12–14]. Previous studies have often treated the Akt family as a single entity that regulates inflammatory responses through the modulation of its upstream and downstream genes [15, 16]. Nevertheless, recent investigations have revealed that different Akt isoforms exert distinct effects on many biological processes, such as cell survival, proliferation, and differentiation [17, 18]. Akt2 is one of the three closely related serine/threonine-protein kinases in the Akt family. Many studies have suggested that inhibition of Akt2 induces macrophage M2 phenotype polarization and locally reverses the proinflammatory microenvironment [19–21]. However, the regulatory role of Akt2 and its potential mechanism in ADD and TMJOA have not been reported. Our earlier work revealed that Akt2 inhibition could reduce osteoclast formation and attenuate condylar subchondral bone loss in early-stage ADD-induced TMJOA [22], but whether Akt2 inhibition could improve condylar bone morphology and alleviate cartilage degeneration has yet to be determined.

As such, this study aimed to determine the role and underlying mechanism of the Akt2 pathway in different stages of ADD. We hypothesized that selective inhibition of Akt2 could alleviate the progression of ADD-induced TMJOA by preventing condylar subchondral bone loss. To assess this hypothesis, we established a rat ADD model, Akt2 was knocked down, the expression and location of phosphorylated Akt2 in different stages of ADD were investigated, and the pathological changes and potential mechanisms involved were elucidated.

Methods

Animal model

Eight-week-old male Sprague–Dawley rats were purchased from Vital River Laboratory (China). All the animals were fed in a specific pathogen-free environment with a 12 h light/dark cycle at room temperature and easy access to food and water. For determination of the pathological changes in different stages of ADD-induced TMJOA, the rats were randomly divided into the sham and ADD groups ($n = 3$).

For induction of ADD, the rats were anesthetized via an intraperitoneal injection of 1% pentobarbital sodium. Under sterile surgical conditions, the right TMJ was exposed. In the experimental group, a sterile silk suture (5–0) was passed through the posterior band of the disc vertically and anchored to the bend point of the zygomatic arch, which displaced the disc from the upper surface to the anterior surface of the condyle. In the sham group, the disc was separated from the condyle but not displaced.

Adeno-associated virus (AAV) infection

For specific knockdown of Akt2 in rats, an AAV carrying Akt2 shRNA (shAkt2) or negative control (shCtrl) (Genechem Ltd., China) was injected intravenously on the 10th day before surgery. For evaluation of the effects of Akt2 inhibition, the rats were randomly divided into 3 groups ($n = 5$): the sham + shCtrl, ADD + shCtrl, and ADD + shAkt2 groups. The rats were euthanized at 1 week or 8 weeks after surgery. The transfection efficacy of the AAVs was routinely assessed *via* Western blotting and immunofluorescence staining (Supplementary Figs. 1, 2).

Magnetic resonance imaging (MRI)

MRI was used to confirm whether the TMJ disc had undergone anterior displacement after surgery. The rats were first anesthetized with isoflurane (5% for induction and 1% for maintenance) and O_2. Then, pentobarbital sodium (0.05 mg/kg) was injected intraperitoneally. The MR images of the TMJs were acquired on a 9.4T Bruker system (PharmaScan, Bruker, Germany) with an 86 mm volume coil for transmission and a 2 cm × 2 cm phased-array surface coil to receive the signal (ParaVision Version 7.0.0 for MRI acquisitions). After the magnetic field homogeneity was optimized, TurboRARE T2-weighted anatomical images were acquired with the following parameters: repetition time = 3000 ms; echo time = 34 ms; field of view = 25 × 25 mm^2; voxel size = 0.065 × 0.065 × 0.4 mm^3; and total acquisition time = 1152 s.

Microcomputed tomography (micro-CT)

Micro-CT was used to analyze condylar subchondral bone mass according to our previously reported method [22]. In brief, the TMJs were fixed in 10% formalin overnight and scanned at 80 kV, 500 μA, and 33.658 μm pixel size (Inveon, Siemens, Germany). Radiographs were reconstructed and analyzed with Inveon Research Workplace software. Given that the most obvious TMJOA bone changes occurred in the condylar head region (especially the condylar surface), the region of interest covering the condylar head and a total of 70 consecutive cross-sectional images from the most superior point of the condylar head were utilized.

Hematoxylin and eosin staining and immunological staining

The TMJ samples were cut into 5-μm paraffin sections for hematoxylin and eosin (H&E), toluidine blue (TB) and immunohistochemical staining and into 10-μm frozen sections for immunofluorescence staining. H&E staining and TB staining were performed following the instructions of the staining kits (Solarbio Science and Technology, Ltd., China). The modified Mankin scoring system was used to evaluate cartilage and bone deterioration [23]. Immunohistochemical and immunofluorescence staining were performed as described in our previous study [22]. Antibodies against CD68 (Bio-Rad, USA), CTSK (Abcam, USA), and OCN (R&D, USA) were used to observe subchondral bone remodeling; COL2A1 (Novus Biologicals, USA), MMP3 (Proteintech, China), and cleaved caspase-3 (Cell Signaling Technology, USA) antibodies were used to observe cartilage degenerative status; and a *p*-Akt2 (Bioss, China) antibody was used to visualize the expression and location of *p*-Akt2 in TMJs.

Western blot

Condylar cartilage or subchondral bone tissues were lysed in RIPA lysis buffer (Solarbio) supplemented with phenylmethylsulfonyl fluoride and a protease and phosphatase inhibitor (Sigma–Aldrich). The lysates were centrifuged at 12,000 × *g* for 30 min at 4 °C. Then, the total protein concentration was measured with a bicinchoninic acid (BCA) protein assay kit (Thermo Scientific, USA). An aliquot of protein was subjected to SDS–PAGE and transferred electrophoretically to polyvinylidene fluoride membranes (Millipore, USA). After being blocked with 5% bovine serum albumin, the membranes containing the cartilage tissue lysates were incubated at 4 °C overnight with primary antibodies against cleaved caspase-3, caspase-3, MMP3, COL2A1, and β-actin. The membranes containing bone tissue lysates were incubated with antibodies against Akt2, COL1A1, OCN, and β-actin. After washing, the blots were probed with HRP-conjugated secondary antibodies at room temperature for 1 h and subjected to enhanced chemiluminescence detection (Thermo Fisher Scientific). The intensity of each band was quantified by ImageJ and normalized to the density of the internal control.

Statistical analysis

The data are expressed as the means ± standard errors of the means (SEMs). The experiments were repeated at least 3 times. One-way ANOVA with a post hoc Bonferroni's multiple comparison test or an unpaired *t* test was employed to analyze these datasets (Prism 7.0, GraphPad Software, USA). Differences were considered statistically significant at *P* values < 0.05.

Results

Subchondral bone loss precedes condylar degenerative changes in the early stage of ADD

To clarify the pathological changes in the condylar cartilage and subchondral bone after disc displacement, we established a rat ADD model and histologically observed the progression of ADD. Through MRI of the TMJs immediately after surgery, we confirmed that the TMJ disc was displaced anteriorly to the condyle after ADD surgery (Supplementary Fig. 3). Condylar subchondral bone loss occurred rapidly within the first week after ADD surgery, manifesting as condylar cortex discontinuity and condylar surface erosion, which resembled early-stage TMJOA-related bone changes in humans (Fig. 1A). Micro-CT analysis showed lower values of bone mineral density (BMD) and trabecular thickness (Tb.Th) in the ADD group than in the sham group (Fig. 1B, C). In addition, the numbers of $CD68^+$ macrophages and $CTSK^+$ osteoclasts in the osteochondral junction, which are considered early-stage TMJOA changes, were increased in the ADD 1w group (Fig. 1D-G). At 8 weeks after ADD surgery, the modified Mankin score, which is used to evaluate cartilage and bone deterioration of the TMJ, increased (Fig. 2A-C). Western blot analysis revealed that the level of matrix metalloproteinase-3 (MMP3) gradually increased as early as 2 weeks and persisted until 8 weeks after ADD surgery, whereas the number of apoptotic chondrocytes dramatically increased 8 weeks later (Fig. 2D-F). Moreover, immunohistochemical staining verified that the number of cleaved caspase-3-positive cells and MMP3-positive cells in the cartilage increased (Fig. 2G-J). In addition, micro-CT analysis revealed that both BMD and Tb.Th increased (Fig. 1A-C), and the number of OCN^+ osteoblasts in subchondral bone also increased 8 weeks later (Fig. 2K, L), which indicated that degenerative changes such as cartilage degradation and excessive bone formation dominated in this stage. Taken together, these data suggest that subchondral bone loss precedes degenerative changes in condylar cartilage and subchondral bone in the ADD model.

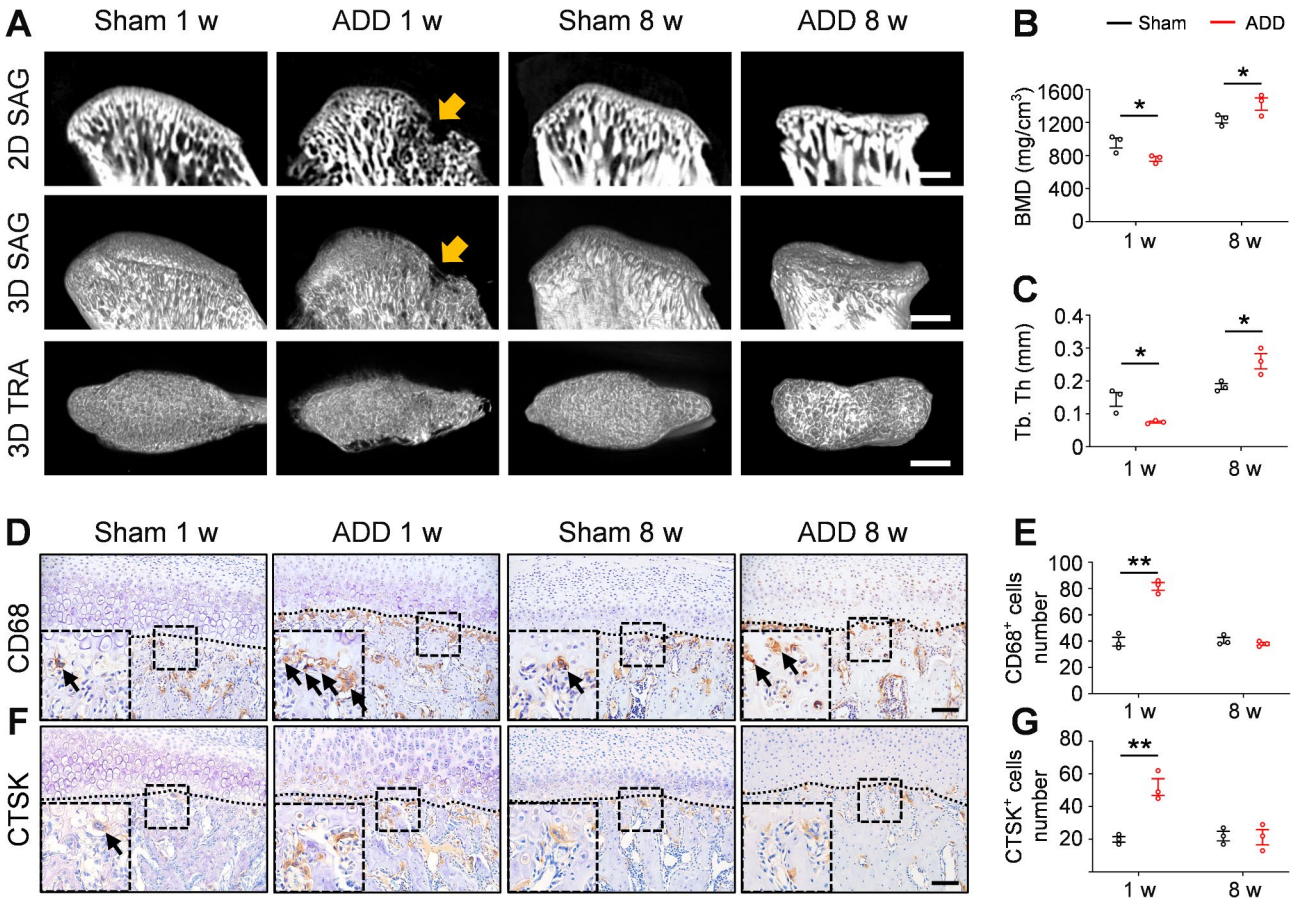

Fig. 1 Condylar subchondral bone loss was rapidly occurred in the early stage of ADD. (**A**) Micro-CT images of the condyles at 1-week and 8-week after sham or ADD surgery. The yellow arrows show articular surface erosion. Scale bar: 1 mm. (**B**, **C**) Quantitative analysis of BMD (**B**) and Tb.Th (**C**) in subchondral bone of the TMJ condylar heads determined by micro-CT measurements at 1-week and 8-week after sham or ADD surgery. Statistical analysis was determined by one-way ANOVA with Bonferroni's multiple comparison test. (**D**, **E**) Representative images (**D**) and quantitative analysis (**E**) of $CD68^+$ cells in subchondral bone of condyles at 1-week and 8-week after sham or ADD surgery. The black dotted line represents the demarcation between articular cartilage and subchondral bone. Scale bar: 100 μm. (**F**, **G**) Representative images (**F**) and quantitative analysis (**G**) of $CTSK^+$ cells in subchondral bone of condyles at 1-week and 8-week after sham or ADD surgery. The black dotted line represents the demarcation between articular cartilage and subchondral bone. Scale bar: 100 μm. The data were presented as mean and SEM. Unpaired *t* test was used to compare the differences between sham and ADD surgery at the same time point. * $P < 0.05$. ** $P < 0.01$. $n = 3$ per group

The Akt2 pathway is activated in subchondral bone macrophages in the early stage of ADD

To study the activation of the Akt2 pathway in TMJs in vivo, we observed the expression and location of *p*-Akt2 via immunohistochemistry. As shown in Fig. 3A-F, the number of *p*-Akt2-positive cells, primarily in subchondral bone, significantly increased in the rat model at 1 week after ADD, with subchondral bone loss, indicating early-stage TMJOA. Additionally, immunofluorescence costaining revealed that the number of *p*-Akt2 and CD68 double-positive cells was significantly increased in the subchondral bone at 1 week after ADD surgery, indicating that the Akt2 pathway was activated in subchondral bone macrophages in the early stage of ADD (Fig. 3G, H).

Akt2 inhibition prevents subchondral bone loss in the early stage of ADD

Our previous study demonstrated that the Akt2 pathway plays essential roles in osteoclast precursor cell differentiation and mature osteoclast bone resorption [22]. Therefore, we investigated the effects of shAkt2 in the early stage of ADD. Micro-CT analysis revealed that, compared with those in the shCtrl-treated group, subchondral bone loss was partially attenuated in the shAkt2-treated group 1 week after ADD, with higher values of BMD, the ratio of bone volume to tissue volume (BV/TV), and Tb.Th but lower values of the ratio of bone surface area to bone volume (BS/BV) (Fig. 4A-E). Furthermore, the secretion of CTSK, which is involved in osteoclast formation and bone resorption, was decreased in the osteochondral junction 1 week after ADD in the shAkt2-treated rats (Fig. 4F, G).

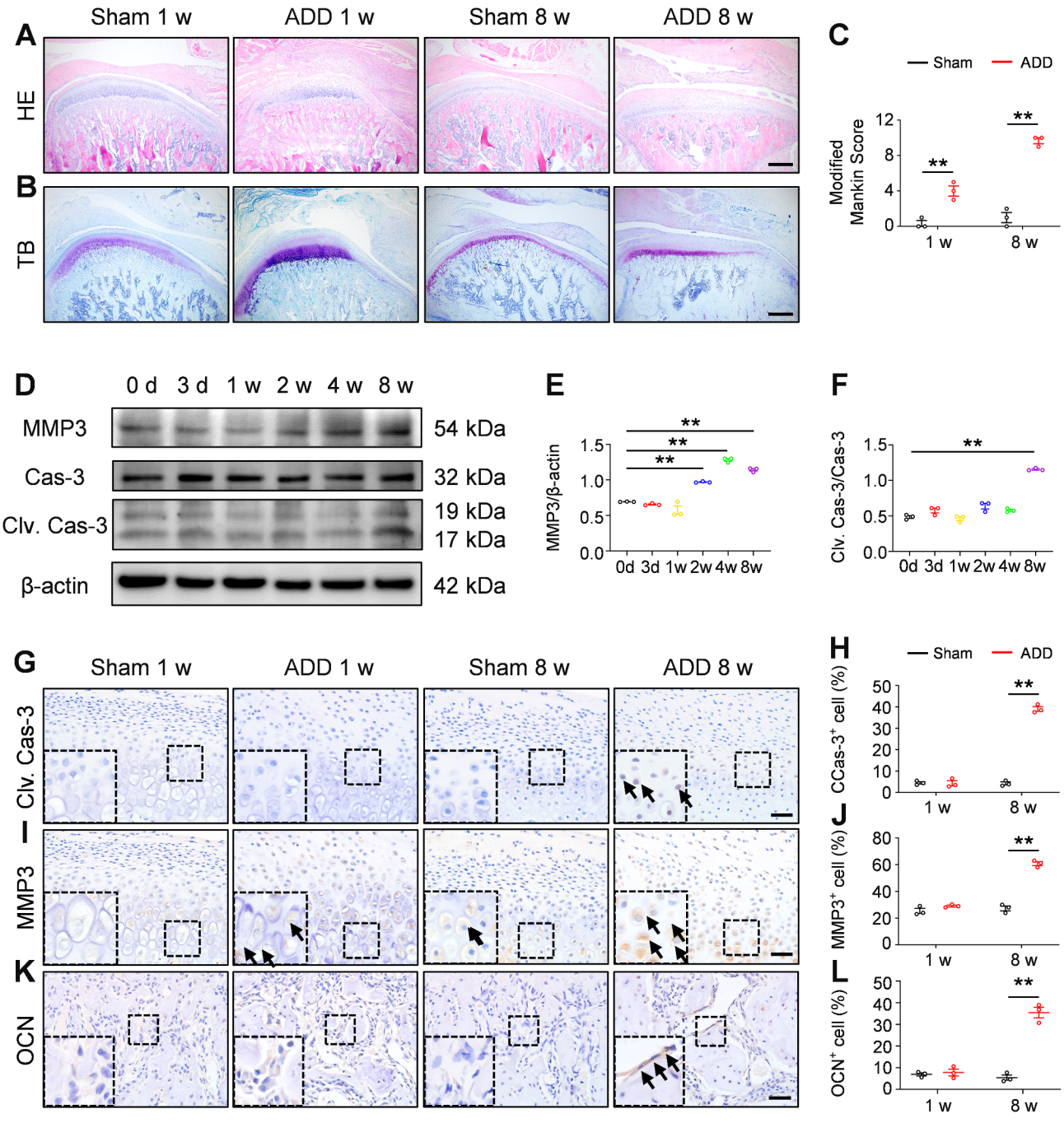

Fig. 2 Condylar cartilage degeneration occurred in the advanced stage of ADD. (**A**) Representative images of H&E staining in TMJ sagittal sections at 1-week and 8-week after sham or ADD surgery. Scale bar: 500 μm. (**B**) Representative images of TB staining in TMJ sagittal sections at 1-week and 8-week after sham or ADD surgery. Scale bar: 500 μm. (**C**) Quantitative analysis of modified Mankin score of condyles at 1-week and 8-week after sham or ADD surgery. (**D**) Representative Western blotting bands showing the expression of MMP3, Cas-3, Clv. Cas-3, and β-actin in condylar cartilage at different time points after ADD surgery. The time points from left to right: 0 days (baseline), 3 days, 1 week, 2 weeks, 4 weeks, and 8 weeks. (**E**, **F**) Quantitative analysis of the relative intensity of MMP3 (**E**) and Clv. Cas-3 (**F**). The level of MMP3 was normalized to β-actin. The level of Clv. Cas-3 was normalized to Cas-3. Statistical analysis was determined by one-way ANOVA with Bonferroni's multiple comparison test. (**G**, **H**) Representative images (**G**) and quantitative analysis (**H**) of Clv. Cas-3$^+$ cells in condylar cartilage at 1-week and 8-week after sham or ADD surgery. Scale bar: 50 μm. (**I**, **J**) Representative images (**I**) and quantitative analysis (**J**) of MMP3$^+$ cells in condylar cartilage at 1-week and 8-week after sham or ADD surgery. Scale bar: 50 μm. (**K**, **L**) Representative images (**K**) and quantitative analysis (**L**) of OCN$^+$ cells in condylar cartilage at 1-week and 8-week after sham or ADD surgery. Scale bar: 50 μm. The data were presented as mean and SEM. Unpaired *t* test was used to compare the differences between sham and ADD surgery at the same time point. ** $P < 0.01$. $n = 3$ per group

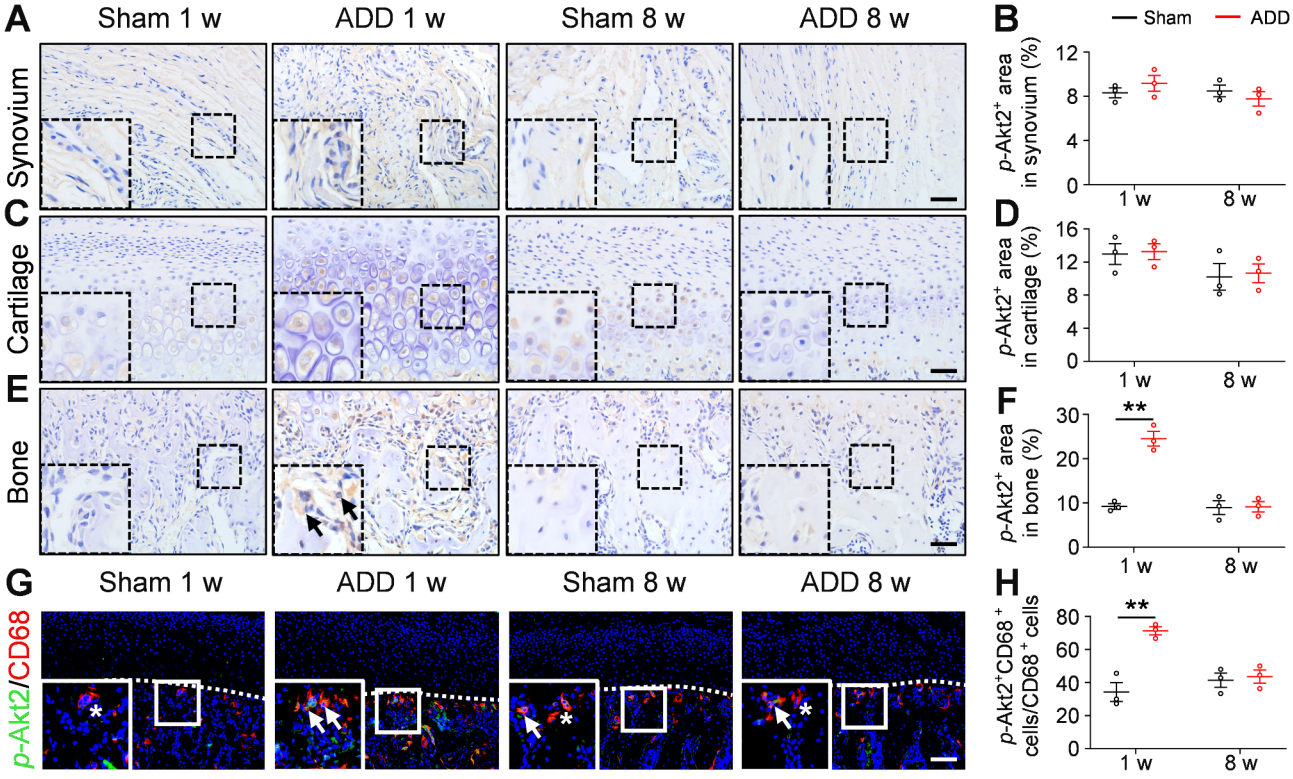

Fig. 3 Akt2 pathway is activated in subchondral bone macrophages in the early stage of ADD. (**A**, **B**) Representative images (**A**) and quantitative analysis (**B**) of *p*-Akt2$^+$ area in synovium at 1-week and 8-week after sham or ADD surgery. Scale bar: 50 μm. (**C**, **D**) Representative images (**C**) and quantitative analysis (**D**) of *p*-Akt2$^+$ area in cartilage at 1-week and 8-week after sham or ADD surgery. Scale bar: 50 μm. (**E**, **F**) Representative images (**E**) and quantitative analysis (**F**) of *p*-Akt2$^+$ area in subchondral bone at 1-week and 8-week after sham or ADD surgery. Scale bar: 50 μm. (**G**) Representative images of *p*-Akt2 and CD68 immunofluorescence co-staining in sagittal views of condyles at 1-week and 8-week after sham or ADD surgery. *p*-Akt2$^+$ cells were presented in green and CD68$^+$ cells were presented in red. The white dotted line represents the demarcation between articular cartilage and subchondral bone. The white arrows indicate *p*-Akt2 and CD68 double-positive cells in subchondral bone, and the asterisks indicate CD68 single-positive cells. Scale bar: 100 μm. (**H**) Quantitative analysis of the ratio of *p*-Akt2 and CD68 double-positive cells to CD68 positive cells in the subchondral bone of the condyle at 1-week and 8-week after sham or ADD surgery. The data were presented as mean and SEM. Unpaired *t* test was used to compare the differences between sham and ADD surgery at the same time point. ** $P < 0.01$. $n = 3$ per group

Akt2 inhibition improves subchondral bone morphology in the advanced stage of ADD

Given the promising anti-bone-resorption function of shAkt2, we explored the potential therapeutic effects of shAkt2 against ADD-induced TMJOA progression in vivo. Eight weeks after ADD surgery, the TMJs developed condylar surface flattening, extensive sclerosis, and joint deformity, which were considered advanced-stage TMJOA bony changes. However, the shAkt2 treatment group presented less abnormal condylar bone remodeling with a reduced severity of sclerosis, and the morphology of the condyles improved. Compared with the shCtrl-treated group, the shAkt2-treated group presented significantly lower values of BMD, BV/TV, and Tb.Th but higher values of BS/BV by 8 weeks after ADD (Fig. 5A-E). In addition, Western blot analysis and immunofluorescence staining revealed that the expression levels of collagen type I and OCN were reduced (Fig. 5F-J), indicating that shAkt2 treatment attenuated bone sclerosis in the advanced stage of ADD.

Akt2 inhibition attenuates articular cartilage degeneration in the advanced stage of ADD

We next assessed whether shAkt2 helps prevent articular cartilage degeneration after ADD surgery. Western blot analysis revealed that cartilage degeneration occurred at 8 weeks after ADD surgery, whereas shAkt2 treatment attenuated cartilage degeneration (Fig. 6A-D). Specifically, compared with those in the shCtrl-treated group, the number of collagen type II-positive cells was increased, and the number of MMP3-positive cells was decreased at 8 weeks after ADD in the shAkt2-treated group, which implied that the degradation of the cartilage extracellular matrix was alleviated (Fig. 6E–G). Immunofluorescence staining revealed that the number of cleaved caspase-3-positive cells in the cartilage decreased significantly, indicating that the number of apoptotic chondrocytes was reduced at 8 weeks after shAkt2 treatment (Fig. 6E, H).

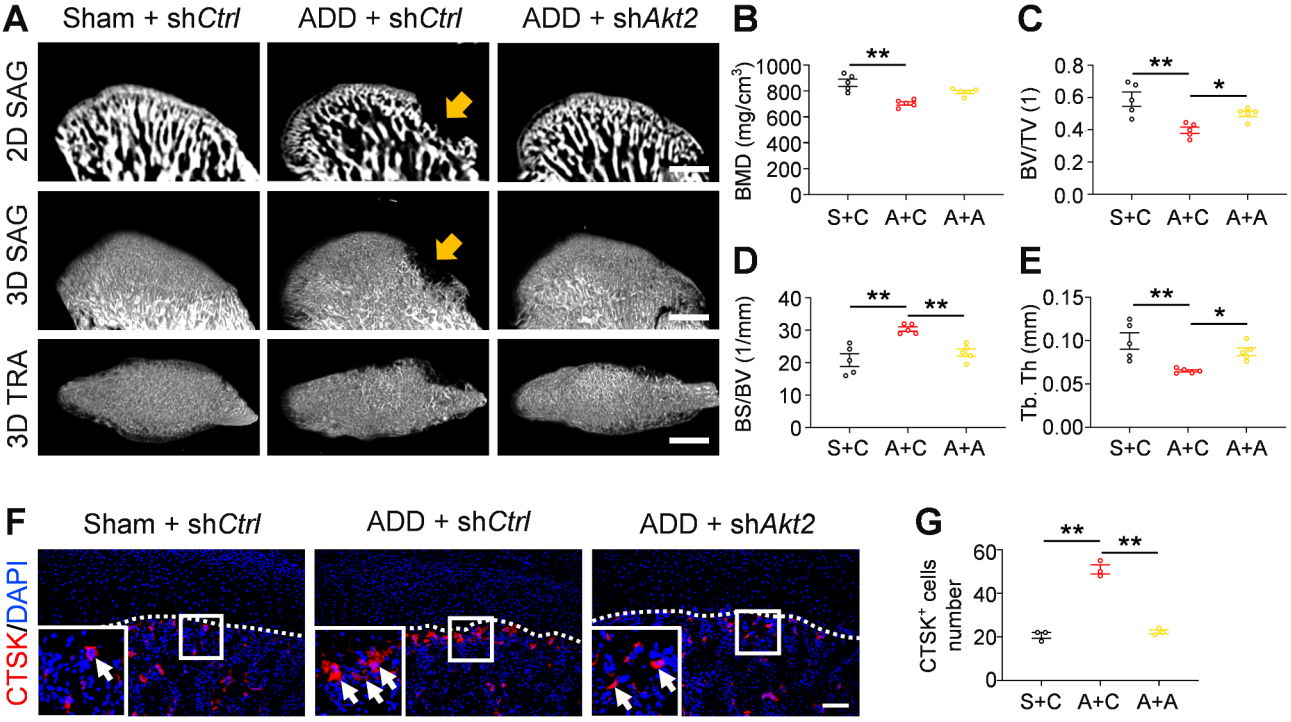

Fig. 4 Specific inhibition of Akt2 prevents subchondral bone loss in the early stage of ADD. (**A**) Micro-CT images of the condyles in the shCtrl- or shAkt2-treated rats at 1-week after receiving sham or ADD surgery. The yellow arrows show articular surface erosion. Scale bar: 1 mm. (**B-E**) Quantitative analysis of BMD (**B**), BV/TV (**C**), BS/BV (**D**), and Tb.Th (**E**) in subchondral bone of the TMJ condylar heads determined by micro-CT measurements in the shCtrl- or shAkt2-treated rats at 1-week after receiving sham or ADD surgery. (**F**, **G**) Representative images (**F**) and quantitative analysis (**G**) of $CTSK^+$ cells in subchondral bone of condyles in shCtrl- or shAkt2-treated rats at 1-week after receiving sham or ADD surgery. The white dotted line represents the demarcation between articular cartilage and subchondral bone. Scale bar: 100 μm. The data were presented as mean and SEM. Statistical analysis was determined by one-way ANOVA with Bonferroni's multiple comparison test. * $P < 0.05$. ** $P < 0.01$. $n = 3–5$ per group

Discussion

In this study, a rat model of ADD-induced TMJOA was established to mimic the pathogenesis of patients in the clinic. The number of osteoclasts increased rapidly with the phosphorylation of Akt2 in subchondral bone macrophages within 1 week post-surgery, which suggested that the activation of Akt2 in macrophages is involved in osteoclast formation. Considering that subchondral bone loss in the early stage might play a vital role in the progression of OA [24, 25], we used shAkt2 to inhibit Akt2 expression and reduce osteoclast formation and subchondral bone loss following ADD surgery. At 8 weeks post-surgery, inhibition of Akt2 improved condylar bone morphology and alleviated cartilage degeneration, which was characterized by a decreased number of apoptotic chondrocytes, reduced expression of various matrix metalloproteinases, and increased type II collagen expression in cartilage tissue. Collectively, these findings indicate that the Akt2 pathway is activated mainly in subchondral bone macrophages during the early stage of ADD and plays an important role in regulating subchondral bone remodeling. Inhibiting Akt2 could alleviate the progression of ADD-induced TMJOA and serve as a potential intervention measure for TMJOA.

Instead of being a chronic disease characterized by cartilage damage, OA is now considered a whole-joint disease that affects various anatomical structures within and around the joint capsule [26]. Emerging evidence has indicated that subchondral bone remodeling is actively involved in the progression of OA and often precedes cartilage degeneration [27–29]. In the early stage of knee OA, there is no evidence of cartilage lesions on the surface of the samples, whereas subchondral bone remodeling is characterized mainly by bone loss [26]. With the development of OA, the subchondral bone morphological structure changes, which cannot provide sufficient stable mechanical support for the upper cartilage, leading to degenerative changes in the stress concentration area of the cartilage [30]. For TMJs, anterior disc displacement without reduction is considered a major cause of the initiation and progression of TMJOA [9, 10]. A previous study revealed that 60–70% of patients presented with early-stage TMJOA manifestations characterized by condylar subchondral bone loss within a year after ADD [10]. Our results are consistent with those of previous studies. Condylar subchondral bone loss occurred rapidly within the first week following ADD-induced TMJOA, with decreased bone mineral density and increased

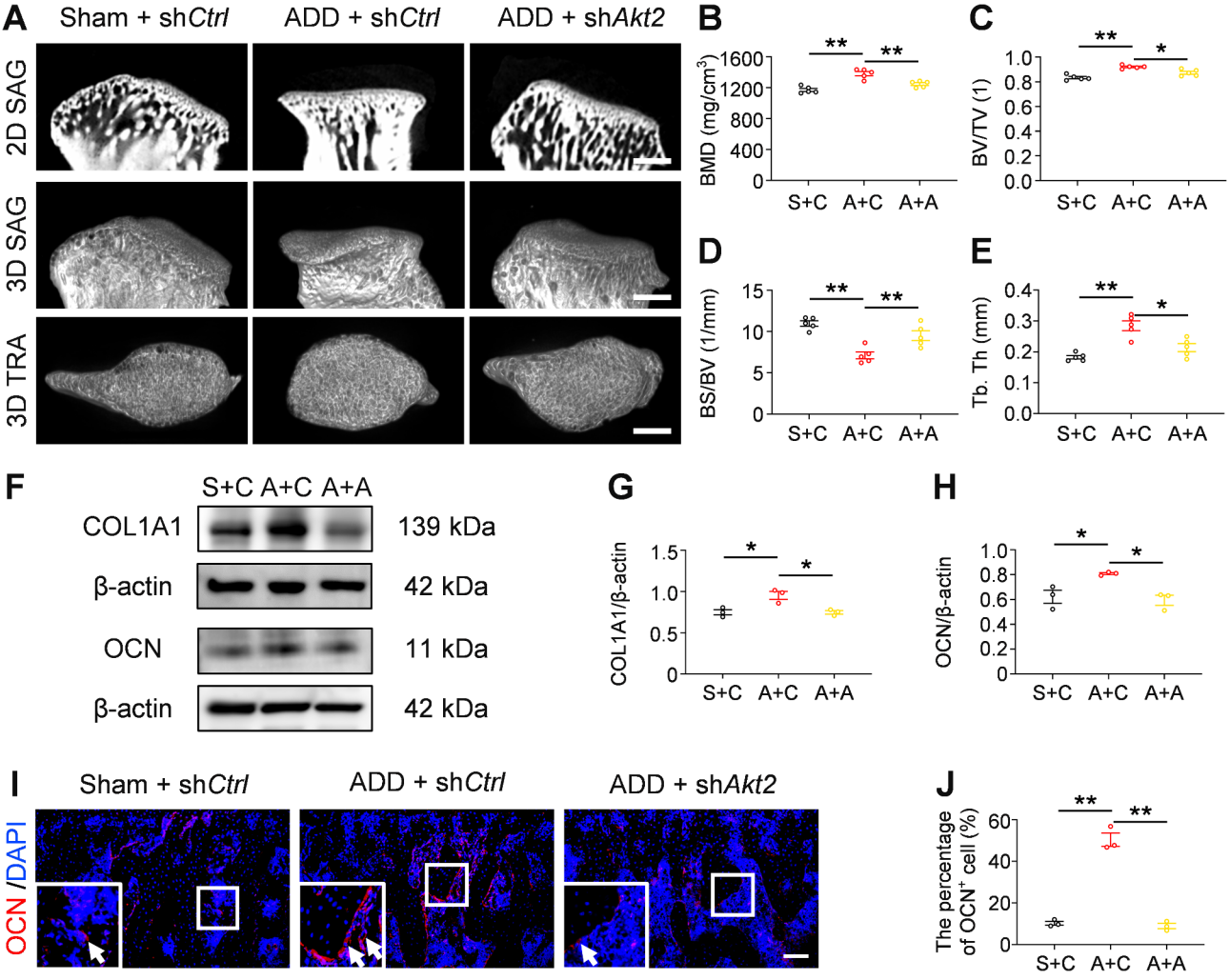

Fig. 5 Specific inhibition of Akt2 improves subchondral bone morphology in the advanced stage of ADD. (**A**) Micro-CT images of the condyles in the shCtrl- or shAkt2-treated rats at 8-week after receiving sham or ADD surgery. Scale bar: 1 mm. (**B-E**) Quantitative analysis of BMD (**B**), BV/TV (**C**), BS/BV (**D**), and Tb.Th (**E**) in subchondral bone of the TMJ condylar heads determined by micro-CT measurements in the shCtrl- or shAkt2-treated rats at 8-week after receiving sham or ADD surgery. (**F**) Representative Western blotting bands showing the expression of COL1A1, OCN, and β-actin in subchondral bone of the condyles in the shCtrl- or shAkt2-treated rats at 8-week after receiving sham or ADD surgery. (**G**, **H**) Quantitative analysis of the relative intensity of COL1A1 (**G**) and OCN (**H**). β-actin was used as an internal control. (**I**, **J**) Representative images (**I**) and quantitative analysis (**J**) of OCN^+ cells in subchondral bone of condyles in shCtrl- or shAkt2-treated rats at 8-week after receiving sham or ADD surgery. The white dotted line represents the demarcation between articular cartilage and subchondral bone. Scale bar: 100 μm. The data were presented as mean and SEM. Statistical analysis was determined by one-way ANOVA with Bonferroni's multiple comparison test. * $P < 0.05$. ** $P < 0.01$. $n = 3–5$ per group

$CTSK^+$ osteoclasts, which play important roles in subsequent cartilage damage, subchondral bone changes, and overall joint degeneration.

As vital components of bone immune regulation, macrophages participate in bone remodeling via phenotypic transformation [31]. On the one hand, macrophages can differentiate into mature osteoclasts and promote bone resorption. On the other hand, macrophages can regulate the inflammatory response and bone remodeling by altering the M1/M2 ratio [32]. Some scholars have revealed that M1 macrophages in the osteoarthritic synovium promote cartilage damage by secreting inflammatory mediators and matrix-degrading enzymes [33–35]. In a rat model of ADD-induced TMJOA, macrophages and osteoclasts residing in the osteochondral junction were significantly increased, and the Akt2 pathway was activated in subchondral bone macrophages in early-stage ADD. Akt2 phosphorylation in macrophages may be involved in the initial stage of bone resorption and thus crucial in regulating bone homeostasis in early-stage ADD-induced TMJOA.

Considering that subchondral bone loss is a typical pathological manifestation of early-stage OA, researchers have attempted to use antiresorptive medications to intervene in the progression of OA [36–39]. Some scholars reported that inhibiting bone remodeling by

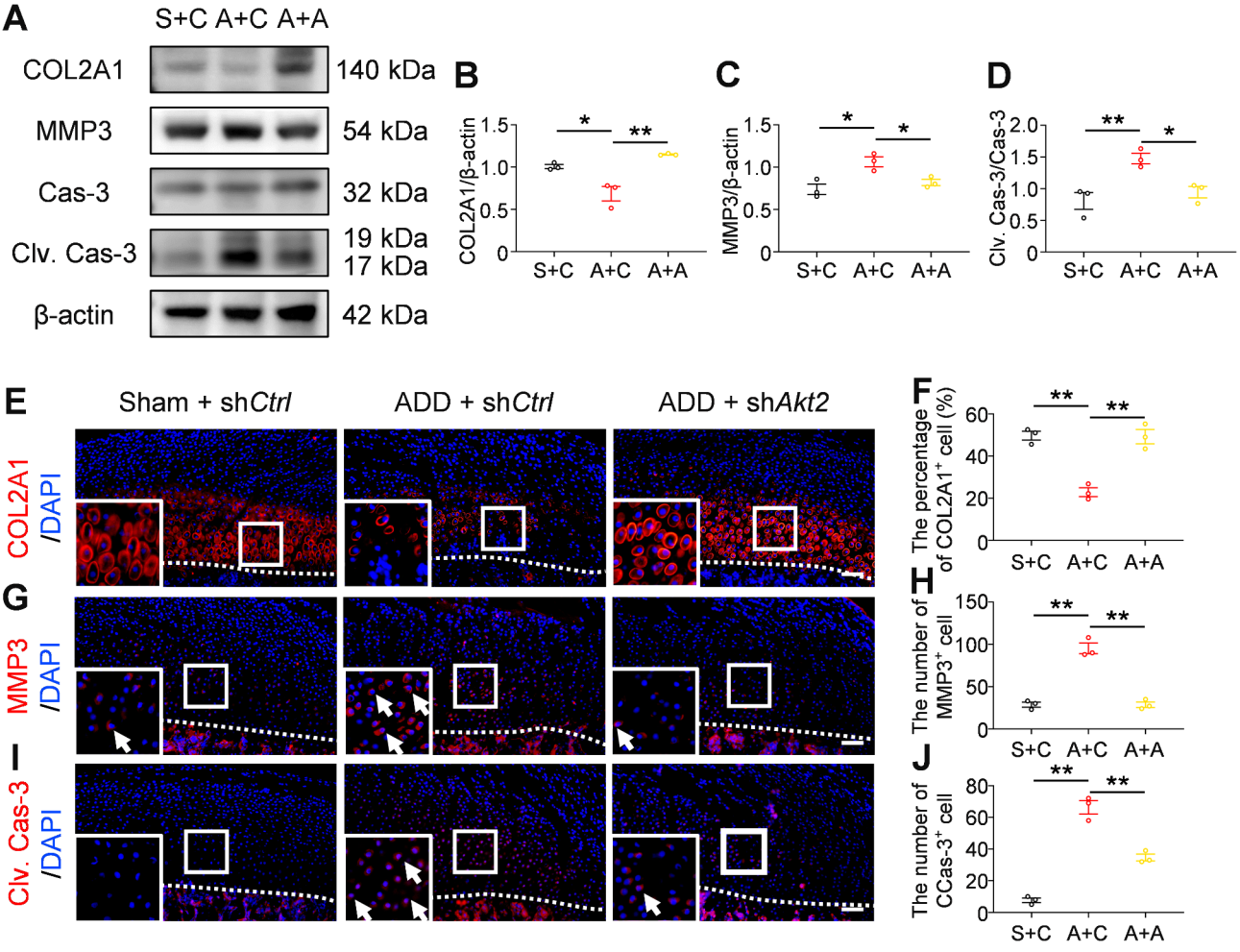

Fig. 6 Specific inhibition of Akt2 attenuates condylar cartilage degeneration in the advanced stage of ADD. (**A**) Representative Western blotting bands showing the expression of COL2A1, MMP3, Cas-3, Clv. Cas-3, and β-actin in cartilage of the condyles in the shCtrl- or shAkt2-treated rats at 8-week after receiving sham or ADD surgery. (**B-D**) Quantitative analysis of the relative intensity of COL1A1 (**B**), MMP3 (**C**), and Clv. Cas-3 (**D**). β-actin was used as an internal control. The level of Clv. Cas-3 was normalized to Cas-3. (**E**, **F**) Representative images (**E**) and quantitative analysis (**F**) of COL2A1$^+$ cells in condylar cartilage in shCtrl- or shAkt2-treated rats at 8-week after receiving sham or ADD surgery. The white dotted line represents the demarcation between articular cartilage and subchondral bone. Scale bar: 100 μm. (**G**, **H**) Representative images (**G**) and quantitative analysis (**H**) of MMP3$^+$ cells in condylar cartilage in shCtrl- or shAkt2-treated rats at 8-week after receiving sham or ADD surgery. The white dotted line represents the demarcation between articular cartilage and subchondral bone. Scale bar: 100 μm. (**I**, **J**) Representative images (**I**) and quantitative analysis (**J**) of Clv. Cas-3$^+$ cells in condylar cartilage in shCtrl- or shAkt2-treated rats at 8-week after receiving sham or ADD surgery. The white dotted line represents the demarcation between articular cartilage and subchondral bone. Scale bar: 100 μm. The data were presented as mean and SEM. Statistical analysis was determined by one-way ANOVA with Bonferroni's multiple comparison test. * $P < 0.05$. ** $P < 0.01$. $n = 3$ per group

alendronate immediately after load-induced post-traumatic osteoarthritis reduced cartilage degeneration and slowed the development of OA-related changes in subchondral bone [40]. Similarly, Hayes et al. reported that bisphosphonates had good therapeutic effects on patients with early-stage knee OA with normal body weight but were not associated with progression in those with advanced-stage OA [41]. These results indicated that inhibiting subchondral bone resorption promptly could maintain subchondral bone mass and reduce cartilage degeneration. However, long-term bisphosphonate use has potential side effects, such as medication-related osteonecrosis [42, 43], and new strategies for inhibiting subchondral bone loss are needed. For confirmation of the effect of Akt2 inhibition on early intervention in ADD-induced TMJOA, rats were intravenously injected with shAkt2 10 days before ADD. Our data revealed that inhibiting Akt2 reduced condylar bone resorption following ADD surgery, improved condylar bone morphology, and alleviated degenerative changes in articular cartilage at 8 weeks post-surgery. To the best of our knowledge, the role of Akt2 in ADD-induced TMJOA has not been previously investigated. Taken together, these findings suggest that Akt2 inhibition could be crucial in regulating bone homeostasis and that Akt2 could be a promising target in the treatment of TMJOA.

The present study has several limitations. shAkt2 can effectively inhibit Akt2 expression, but its clinical application is challenging because of the stability of delivery vectors and the feasibility of large-scale production. In addition, intravenous injection of AAV may alter the inflammatory environment of the entire joint and impact ADD-induced TMJOA development. Next, we need to explore more targeted drugs to specifically inhibit the expression of Akt2 in subchondral bone macrophages. In addition, although Akt2 inhibition could reduce condylar subchondral bone loss in ADD-induced early-stage TMJOA, we were unable to determine the duration of treatment required to attenuate early-stage subchondral bone changes associated with TMJOA. Overall, more studies incorporating targeted drugs, administration methods, and treatment windows are needed to investigate how effectively inhibiting subchondral bone loss inhibits long-term TMJOA progression.

Conclusion

This study revealed that the Akt2 pathway is activated mainly in subchondral bone macrophages during ADD-induced early-stage TMJOA and plays an important role in regulating subchondral bone homeostasis. Akt2 inhibition could alleviate the degenerative changes in articular cartilage and subchondral bone and serve as a prophylactic treatment following ADD to slow TMJOA progression. Future work should seek a targeted drug to better understand the role of subchondral bone loss in ADD-induced TMJOA. A short-term course of treatment following ADD to attenuate or prevent TMJOA progression may be feasible and should be explored.

Abbreviations

OA	Osteoarthritis
TMJ	Temporomandibular joint
ADD	Anterior disc displacement
AAV	Adeno-associated virus
shAkt2	Akt2 shRNA
BCA	Bicinchoninic acid
H&E	Hematoxylin and eosin
TB	Toluidine blue
COL2A1	Collagen type II alpha 1
COL1A1	Collagen type I alpha 1
MMP3	Matrix Metallopeptidase 3
CTSK	Cathepsin K
OCN	Osteocalcin
MRI	Magnetic resonance imaging
CT	Computed tomography
BMD	Bone mineral density
BV/TV	The ratio of bone volume to tissue volume
BS/BV	The ratio of bone surface area to bone volume
Tb. Th	Trabecular thickness
SEM	Standard error of mean

Supplementary Information

The online version contains supplementary material available at https://doi.org/10.1186/s13075-025-03506-x.

Supplementary Material 1

Supplementary Material 2

Acknowledgements

The authors thank the National Center for Protein Sciences at Peking University for assistance with MRI research. We thank Dr. Mengxi Yue and Dr. Xiaohang Liang for their help with MRI data acquisition.

Author contributions

FSY conceived and designed the study, collected the data, evaluated the imaging studies, planned the analysis, and drafted the manuscript. CMN collected the data, evaluated the imaging studies, planned the analysis, and interpreted the data. GCC collected the data, evaluated the imaging studies, and gave input to the analysis. LYX evaluated the imaging studies. LJ and FKY conceived and designed the study, planned the analysis, and revised the manuscript. All authors read and approved the final manuscript and agree to be accountable for the content.

Funding

This work was supported by grants from the National Key R&D Project of China, Ministry of Science and Technology of the People's Republic of China (2023YFC2509200), the National Natural Science Foundation of China (82170979, 82201091), China Postdoctoral Science Foundation (2023M740140), and Peking University Medicine Sailing Program for Young Scholars' Scientific & Technological Innovation (BMU2024YFJHPY002).

Data availability

No datasets were generated or analysed during the current study.

Declarations

Ethics approval and consent to participate

All animal experiments were approved by the Peking University Animal Ethics Committee (PUIRB-LA2023037).

Consent for publication

Not applicable.

Competing interests

The authors declare no competing interests.

Received: 9 August 2024 / Accepted: 15 February 2025
Published online: 27 February 2025

References

1. Allen KD, Thoma LM, Golightly YM. Epidemiology of osteoarthritis. Osteoarthritis Cartilage. 2022;30(2):184–95.
2. Cardoneanu A, Macovei LA, Burlui AM, Mihai IR, Bratoiu I, Rezus II, et al. Temporomandibular Joint Osteoarthritis: pathogenic mechanisms involving the cartilage and subchondral bone, and potential therapeutic strategies for joint regeneration. Int J Mol Sci. 2022;24(1):171.
3. Nickel JC, Iwasaki LR, Gonzalez YM, Gallo LM, Yao H. Mechanobehavior and Ontogenesis of the Temporomandibular Joint. J Dent Res. 2018;97(11):1185–92.
4. Cai S, Zou Y, Zhao Y, Lin H, Zheng D, Xu L, et al. Mechanical stress reduces secreted frizzled-related protein expression and promotes temporomandibular joint osteoarthritis via Wnt/β-catenin signaling. Bone. 2022;161:116445.
5. Zhou J, Ren R, Li Z, Zhu S, Jiang N. Temporomandibular joint osteoarthritis: a review of animal models induced by surgical interventions. Oral Dis. 2023;29(7):2521–8.
6. Yap AU, Lei J, Zhang XH, Fu KY. TMJ degenerative joint disease: relationships between CBCT findings, clinical symptoms, and signs. Acta Odontol Scand. 2023;81(7):562–8.
7. Collin M, Hagelberg S, Ernberg M, Hedenberg-Magnusson B, Christidis N. Temporomandibular joint involvement in children with juvenile idiopathic arthritis-Symptoms, clinical signs and radiographic findings. J Oral Rehabil. 2022;49(1):37–46.

8. Yap AU, Zhang MJ, Cao Y, Lei J, Fu KY. Comparison of Psychological States and oral health-related quality of life of patients with Differing Severity of Temporomandibular disorders. J Oral Rehabil. 2022;49(2):177–85.
9. Bi R, Li Q, Li H, Wang P, Fang H, Yang X, et al. Divergent chondro/osteogenic transduction laws of fibrocartilage stem cell drive temporomandibular joint osteoarthritis in growing mice. Int J Oral Sci. 2023;15(1):36.
10. Lei J, Han J, Liu M, Zhang Y, Yap AU, Fu KY. Degenerative Temporomandibular Joint Changes Associated with recent-onset disc displacement without reduction in adolescents and young adults. J Craniomaxillofac Surg. 2017;45(3):408–13.
11. Juan Z, Xing-Tong M, Xu Z, Chang-Yi L. Potential pathological and molecular mechanisms of temporomandibular joint osteoarthritis. J Dent Sci. 2023;18(3):959–71.
12. Glaviano A, Foo ASC, Lam HY, Yap KCH, Jacot W, Jones RH, et al. PI3K/AKT/mTOR signaling transduction pathway and targeted therapies in cancer. Mol Cancer. 2023;22(1):138.
13. Acosta-Martinez M, Cabail MZ. The PI3K/Akt pathway in Meta-inflammation. Int J Mol Sci. 2022;23(23):15330.
14. Sun K, Luo J, Guo J, Yao X, Jing X, Guo F. The PI3K/AKT/mTOR signaling pathway in osteoarthritis: a narrative review. Osteoarthritis Cartilage. 2020;28(4):400–9.
15. Vergadi E, Ieronymaki E, Lyroni K, Vaporidi K, Tsatsanis C. Akt signaling pathway in macrophage activation and M1/M2 polarization. J Immunol. 2017;198(3):1006–14.
16. He X, Li Y, Deng B, Lin A, Zhang G, Ma M, et al. The PI3K/AKT signalling pathway in inflammation, cell death and glial scar formation after traumatic spinal cord injury: mechanisms and therapeutic opportunities. Cell Prolif. 2022;55(9):e13275.
17. Arranz A, Doxaki C, Vergadi E, Martinez de la Torre Y, Vaporidi K, Lagoudaki ED, et al. Akt1 and Akt2 protein kinases differentially contribute to macrophage polarization. Proc Natl Acad Sci U S A. 2012;109(24):9517–22.
18. Cole PA, Chu N, Salguero AL, Bae H. AKTivation mechanisms. Curr Opin Struct Biol. 2019;59:47–53.
19. Ieronymaki E, Theodorakis EM, Lyroni K, Vergadi E, Lagoudaki E, Al-Qahtani A, et al. Insulin Resistance in Macrophages alters their metabolism and promotes an M2-Like phenotype. J Immunol. 2019;202(6):1786–97.
20. Wu X, Chen H, Wang Y, Gu Y. Akt2 affects Periodontal inflammation via altering the M1/M2 ratio. J Dent Res. 2020;99(5):577–87.
21. Yin J, Hu T, Xu L, Zhang L, Zhu J, Ye Y, et al. Hsa_circRNA_103124 upregulation in Crohn's disease promoted macrophage M1 polarization to maintain an inflammatory microenvironment via activation of the AKT2 and TLR4/NF-κB pathways. Int Immunopharmacol. 2023;123:110763.
22. Feng SY, Lei J, Li YX, Shi WG, Wang RR, Yap AU, et al. Increased joint loading induces subchondral bone loss of the temporomandibular joint via the RANTES-CCRs-Akt2 axis. JCI Insight. 2022;7(21):e158874.
23. Moskowitz RW. Osteoarthritis cartilage histopathology: grading and staging. Osteoarthritis Cartilage. 2006;14(1):1–2.
24. Wang H, Yuan T, Wang Y, Liu C, Li D, Li Z, et al. Osteoclasts and osteoarthritis: novel intervention targets and therapeutic potentials during aging. Aging Cell. 2024;23(4):e14092.
25. Klose-Jensen R, Hartlev LB, Boel LWT, Laursen MB, Stengaard-Pedersen K, Keller KK, et al. Subchondral bone turnover, but not bone volume, is increased in early stage osteoarthritic lesions in the human hip Joint. Osteoarthritis Cartilage. 2015;23(12):2167–73.
26. Hugle T, Geurts J. What drives osteoarthritis?-Synovial Versus Subchondral Bone Pathology. Rheumatology (Oxford). 2017;56(9):1461–71.
27. Hu W, Chen Y, Dou C, Dong S. Microenvironment in subchondral bone: Predominant Regulator for the treatment of Osteoarthritis. Ann Rheum Dis. 2021;80(4):413–22.
28. Hu Y, Chen X, Wang S, Jing Y, Su J. Subchondral bone microenvironment in Osteoarthritis and Pain. Bone Res. 2021;9(1):20.
29. Zhu S, Zhu J, Zhen G, Hu Y, An S, Li Y, et al. Subchondral bone osteoclasts induce sensory innervation and Osteoarthritis Pain. J Clin Invest. 2019;129(3):1076–93.
30. Goldring SR, Goldring MB. Changes in the Osteochondral Unit during Osteoarthritis: structure, function and Cartilage-Bone Crosstalk. Nat Rev Rheumatol. 2016;12(11):632–44.
31. Hu K, Shang Z, Yang X, Zhang Y, Cao L. Macrophage polarization and the regulation of bone immunity in bone homeostasis. J Inflamm Res. 2023;16:3563–80.
32. Sun Y, Li J, Xie X, Gu F, Sui Z, Zhang K, et al. Macrophage-Osteoclast associations: Origin, polarization, and subgroups. Front Immunol. 2021;12:778078.
33. Zhang H, Cai D, Bai X. Macrophages regulate the progression of osteoarthritis. Osteoarthritis Cartilage. 2020;28(5):555–61.
34. Yuan Z, Jiang D, Yang M, Tao J, Hu X, Yang X, et al. Emerging roles of macrophage polarization in Osteoarthritis: mechanisms and therapeutic strategies. Orthop Surg. 2024;16(3):532–50.
35. Wu CL, Harasymowicz NS, Klimak MA, Collins KH, Guilak F. The role of macrophages in osteoarthritis and cartilage repair. Osteoarthritis Cartilage. 2020;28(5):544–54.
36. Zhu X, Chan YT, Yung PSH, Tuan RS, Jiang Y. Subchondral bone remodeling: a therapeutic target for Osteoarthritis. Front Cell Dev Biol. 2020;8:607764.
37. Bei MJ, Tian FM, Xiao YP, Cao XH, Liu N, Zheng ZY, et al. Raloxifene retards cartilage degradation and improves subchondral bone micro-architecture in Ovariectomized rats with Patella Baja-Induced-Patellofemoral Joint Osteoarthritis. Osteoarthritis Cartilage. 2020;28(3):344–55.
38. Pang C, Wen L, Lu X, Luo S, Qin H, Zhang X, et al. Ruboxistaurin maintains the bone Mass of Subchondral Bone for blunting osteoarthritis progression by inhibition of Osteoclastogenesis and bone resorption activity. Biomed Pharmacother. 2020;131:110650.
39. Ziemian SN, Witkowski AM, Wright TM, Otero M, van der Meulen MCH. Early inhibition of subchondral bone remodeling slows load-Induced Posttraumatic Osteoarthritis Development in mice. J Bone Min Res. 2021;36(10):2027–38.
40. Ding D, Wang L, Yan J, Zhou Y, Feng G, Ma L, et al. Zoledronic acid generates a spatiotemporal effect to attenuate osteoarthritis by inhibiting potential Wnt5a-associated abnormal subchondral bone resorption. PLoS ONE. 2022;17(7):e0271485.
41. Hayes KN, Giannakeas V, Wong AKO. Bisphosphonate use is protective of Radiographic knee osteoarthritis progression among those with low Disease Severity and being non-overweight: data from the Osteoarthritis Initiative. J Bone Min Res. 2020;35(12):2318–26.
42. Ruggiero SL, Dodson TB, Aghaloo T, Carlson ER, Ward BB, Kademani D. American Association of Oral and maxillofacial surgeons' position paper on medication-related osteonecrosis of the Jaws-2022 Update. J Oral Maxillofac Surg. 2022;80(5):920–43.
43. Nogueira D, Caldas IM, Dinis-Oliveira RJ. Bisphosphonates and osteonecrosis of the jaws: clinical and forensic aspects. Arch Oral Biol. 2023;155:105792.

Publisher's note